Phonon-induced dephasing of chromium color centers in diamond

T. Müller,[1] I. Aharonovich,[2] Z. Wang,[3] X. Yuan,[3] S. Castelletto,[4] S. Prawer,[5] and M. Atatüre[1]
[1]*Cavendish Laboratory, University of Cambridge, JJ Thomson Avenue, Cambridge CB3 0HE, United Kingdom*
[2]*School of Engineering and Applied Science, Harvard University, Cambridge, Massachusetts 02138, USA*
[3]*HFNL and Department of Modern Physics, University of Science and Technology of China, Hefei, 230026, China*
[4]*Centre for Quantum Science and Technology, Department of Physics and Astronomy, Macquarie University, Sydney, New South Wales 2109, Australia*
[5]*School of Physics, University of Melbourne, Melbourne, Victoria 3010, Australia*
(Received 27 August 2012; revised manuscript received 23 October 2012; published 30 November 2012)

We report on the coherence properties of single photons from chromium-based color centers in diamond. We use field-correlation and spectral line-shape measurements to reveal the interplay between slow spectral wandering and fast dephasing mechanisms as a function of temperature. The zero-phonon transition frequency and its linewidth follow a power-law dependence on temperature, which is consistent with direct electron-phonon coupling and phonon-modulated Coulomb coupling to nearby impurities, which are the predominant fast dephasing mechanisms for these centers. Further, the observed reduction in the quantum yield for photon emission as a function of temperature suggests the opening of additional nonradiative channels through thermal activation to higher-energy states and indicates a near-unity quantum efficiency at 4 K.

DOI: 10.1103/PhysRevB.86.195210 PACS number(s): 61.72.J−, 81.05.ug

I. INTRODUCTION

Diamond plays a key role in a wide range of applications in both electronics[1] and photonics[2] today. Due to its wide band gap it hosts a variety of optically active centers in the visible and the near-infrared parts of the spectrum.[3] The nitrogen-vacancy (NV) center has attracted great attention due to its remarkable spin properties as a model system for quantum technologies.[4–6] Other optically active centers, such as silicon-vacancy,[7] nickel,[8] xenon,[9] and chromium,[10] have also shown desirable photonic properties, such as short lifetimes, predominant emission into the zero-phonon line (ZPL), and spectral tuning via the dc Stark effect.[11–13] However, the ZPL spectrum of diamond color centers is typically broader than the radiative linewidth, evidencing the influence of dephasing mechanisms on the optical transitions.[14] These dephasing mechanisms can range from slow spectral wandering of the transition due to charge fluctuations in the environment to fast dephasing processes. The former can be remedied by direct feedback control on the transition, which has been demonstrated for NV centers.[15] The latter is irreversible and presents a fundamental limit to the single-photon coherence even with feedback. Therefore, it is essential to identify the source for these mechanisms, as well as the extent of their contributions to the spectral broadening of these centers. Here, we investigate the dephasing mechanisms influencing the chromium color centers and report that possible sources for fast dephasing are direct electron-phonon coupling and phonon-modulated Coulomb coupling to nearby impurities, which are both consistent with the power-law temperature dependence of the transition frequency and linewidth. Further, the temperature dependence of the quantum yield reveals the existence of a thermal excitation mechanism to higher-energy states similar to the neutral silicon-vacancy centers in diamond.[16]

II. SETUP AND SAMPLE CHARACTERIZATION

Chromium centers can be formed either by chemical vapor deposition (CVD) growth, where the etched sapphire substrate acts as the source for chromium atoms,[17] or by implantation into bulk diamond.[18] While the centers in bulk diamond exhibit narrower emission linewidth than those grown in nano- or microcrystals, they suffer from low photon collection efficiency due to total internal reflection, as well as reduced photostability.[12] We therefore concentrate on centers in microcrystals (size $\sim 2\ \mu$m) for the investigation of dephasing mechanisms. The experimental setup used for the optical measurements is illustrated in Fig. 1(a). A temperature-controlled cryostat and a homemade confocal optical microscope are used to access the centers optically. The chromium centers are excited by a continuous-wave laser at 700 nm, and the emission ($\sim$780 nm) is collected into a single-mode fiber. A time-correlated photon-counting setup is used for excited-state lifetime measurements as well as intensity-correlation measurements. The excited-state lifetimes of chromium centers in bulk, microcrystal, and nanocrystal diamonds can vary significantly.[18,19] Figures 1(b) and 1(c) display exemplary results for these measurements performed at 4 K on a single chromium center in a microcrystal, and the value of 1.7 ns extracted from the measurements is consistent with the range of values reported to date. Based on this value, transform-limited photon emission is expected to result in a coherence time of 3.4 ns. A calibrated and scannable Michelson interferometer and a spectrometer with 8-GHz resolution are used in parallel to quantify the degree of dephasing via the first-order coherence of the photon emission [see Fig. 1(a)].

Figures 2(a) and 2(b) display the measured interference visibility $V = (I_{\max} - I_{\min})/(I_{\max} + I_{\min})$ as a function of relative time delay due to path-length difference for photons from two color centers situated in two different microcrystals (labeled A and B, with ZPL at 756 and 770 nm, respectively). Solid black circles are the experimental data, and the solid red curves are the theoretical fits. Common to both color centers is the coherence time scale approximately 30 times lower than the radiative lifetime. The coherence functions for these centers are, however, fundamentally different from each other. Center

 ©2012 American Physical Society

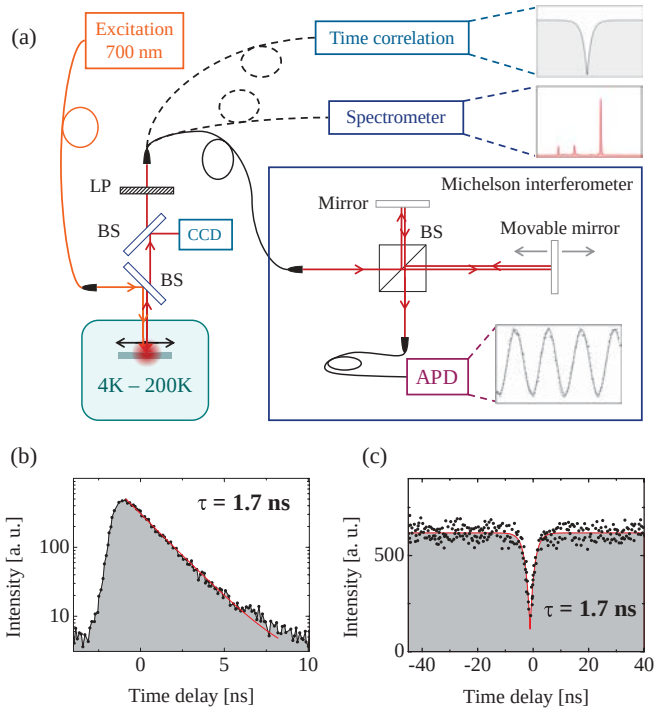

FIG. 1. (Color online) (a) Schematic of the confocal microscope used for the experiments. BS is a beam splitter, and LP is a 740-nm long-pass filter to remove residual laser reflection from luminescence by the chromium emitters. (b) Lifetime measured for the 773.3-nm transition line in the inset in (a). A value of 1.7 ns is extracted from the single exponential fit. (c) Autocorrelation measurement for the 773.3-nm line with $g^{(2)}(0) = 0.28$. This value reflects the finite system response time and background emission from the crystal. The respective fit again reveals an excited state lifetime of 1.7 ns.

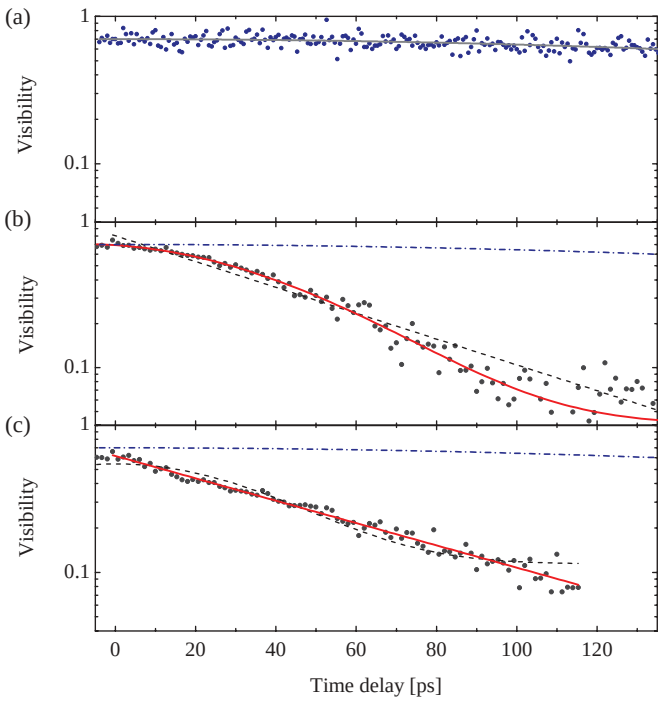

FIG. 2. (Color online) First-order field autocorrelation measurement $g^{(1)}$ performed at liquid-helium temperature (4 K) on centers A and B, as well as a chromium center implanted in bulk diamond. (a) The measured $g^{(1)}$ for a chromium center located in bulk diamond (solid blue circles) display a coherence time longer than 700 ps (solid gray curve). (b) For center A the visibility extracted from interference fringes at different time delays between the two arms of a Michelson interferometer (solid black circles) exhibits a Gaussian decay pattern with a $\tau_{1/e} = 62$ ps (solid red curve). An exponential function is shown for comparison (dotted black curve). The dash-dotted blue curve indicates the coherence time for a center in bulk diamond, as displayed in (a), and is shown for comparison. (c) For center B the extracted visibility (solid black circles) follows an exponential decay profile (solid red curve) with a coherence time of 57 ps. Again, a Gaussian profile (dotted black curve) is shown for comparison along with the fitted curve for the $g^{(1)}$ of the chromium center in bulk diamond (dash-dotted blue curve).

A, shown in Fig. 2(b), displays a predominantly Gaussian decay of coherence (the solid red curve is a Gaussian fit with $\tau_{1/e} = 62$ ps), whereas for center B, shown in Fig. 2(c), the coherence decays exponentially (the solid red curve displays an exponential fit with $\tau_{1/e} = 57$ ps). The exponential form of the coherence function for center B indicates a dominant contribution from the irreversible dephasing mechanisms to the emission spectrum, while the Gaussian-like coherence function of center A limits an exponential contribution to a time scale not shorter than 210 ps. This corresponds to a 750-MHz upper bound to the irreversible broadening for the linewidth for this center. The relatively short coherence times exhibited by both emitters as well as the different profiles in spectra and coherence functions indicate that the immediate environment of the emitters has a varying impact on their photonic properties. In order to emphasize the effect of the environment on photonic coherence, a $g^{(1)}$ measurement performed on a chromium center implanted directly in bulk diamond with lower density of impurities is shown in Fig. 2(a) (solid blue circles). This center shows a ZPL at 790 nm. A coherence time longer than 700 ps is extracted for a Gaussian coherence function (solid gray curve), an order of magnitude longer than the coherence time measured for nanodiamonds.

III. TEMPERATURE DEPENDENCE OF ZPL LINESHAPE

The degree of optical dephasing can be revealed in first-order coherence as well as spectral measurements. If the line broadening is small compared to the natural linewidth, the former is more accurate, whereas for strong dephasing, the latter provides a better means of determining emission linewidths. Figure 3(a) displays the characteristic broadening and redshift of the emission spectrum of another chromium center (labeled center C) as a function of lattice temperature between 9 and 126 K. An analysis of the spectrum reveals that the Gaussian contribution remains constant for all temperatures, while the Lorentzian contribution is temperature dependent. This leads to a switch from a predominantly Gaussian-like line shape at low temperatures to a Lorentzian line shape at higher temperatures for the ten emitters investigated. This can be seen in the linear-log plots of the line shape at two different temperatures displayed in the two insets of Fig. 3(a). The

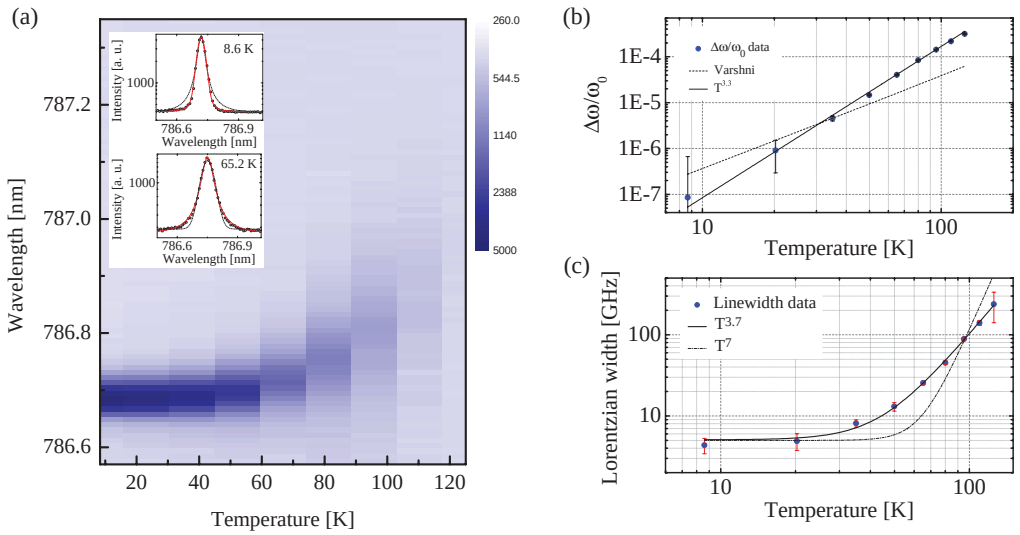

FIG. 3. (Color online) (a) Temperature dependence of an emission line associated with a chromium impurity for lattice temperatures between 8.6 and 125.5 K, with temperature increased in steps of 15 K. The insets are spectra of the emitter plotted on a linear-log scale at 8.6 and 65.2 K, respectively, and demonstrate the transition from a predominantly Gaussian to a predominantly Lorentzian line shape. The red curves are Voigt fits, and the black dotted curves are a Lorentzian curve at 8.6 K and a Gaussian curve at 65.2 K shown for comparison. (b) The shift of center frequency follows a $T^{3.3}$ power law (black solid curve). Varshni temperature dependence is shown for comparison (black dotted curve). (c) Transition linewidth as a function of temperature (blue circles). The linewidth follows a $T^{3.7}$ power law (black solid fit), and a T^7 dependence is shown for comparison.

diamond band gap itself will be modified as a function of temperature, following Varshni's law,[20,21] and shallow centers will inherit this behavior. Figure 3(b) displays the fractional change of the transition frequency ($\Delta\omega/\omega$) as a function of temperature, following a power law of the form $\Delta\omega/\omega \propto T^{\alpha}$ with $\alpha = 3.3$. This frequency shift is distinctly stronger than the Varshni temperature dependence of band gap energy for diamond, as is evident in Fig. 3(b) (black dotted curve). This reveals that all optically relevant states are sufficiently far in energy from the band edges, as expected for deep defects in diamond. Figure 3(c) shows the temperature dependence of the linewidth γ of the Lorentzian contribution to the emission spectrum of center C, following a power law of the form $\gamma \propto T^{\beta}$, with $\beta = 3.7$. These measurements were repeated for ten separate centers, and the average values of α and β are 3.55 and 3.46, respectively, with a standard deviation of 0.5 each. We note that these values compare well with recent temperature-dependence measurements on the silicon-vacancy center: T^3 and $aT^2 + bT^4$ laws are reported for the emission linewidth and the frequency shift as a function of temperature.[24] In the low-temperature regime our data suggest that a temperature-independent dephasing mechanism is present for this center, limiting the linewidth to 4 ± 1 GHz. This residual linewidth varies from center to center and was determined using the Lorentzian width of a Voigt fit to the spectrum, with the Gaussian part being the system response of the spectrometer (~8 GHz). While the error bar for a linewidth below spectrometer resolution is large, the value is clearly above the lifetime broadened limit. Furthermore, it is consistent with the linewidth extracted from the $g^{(1)}$ measurements.

A strong candidate for such a temperature-dependent broadening mechanism is the interaction with lattice phonons. The simplest model for electron-phonon coupling considers quasielastic scattering of phonons with a Debye density of states[22] from a nondegenerate transition of a center. This model predicts a T^7 dependence for dephasing and a T^4 dependence for the fractional change of the transition frequency. The strong deviation of the β values for chromium centers from the prediction by this model suggests the presence of an additional mechanism for temperatures below the Debye temperature T_D. An example of this is already seen in the NV linewidth, which exhibits a T^5 behavior in ultrapure diamond due to the Jahn-Teller effect in the excited states.[23] Further, experimentally determined values of $\alpha = 3.1$ and $\beta = 3$ have been reported for the N3 color center related to nitrogen aggregates in diamond.[25] The particular temperature dependence was attributed to a pronounced deviation of the actual phonon density of states in diamond from the Debye model,[26] which was confirmed experimentally for the N3 color center using the vibrational structure in the N3 absorption spectrum. A numerical evaluation of linewidth and transition frequency shift using the modified phonon density of states in bulk diamond as a function of temperature according to Ref. 22 results in $\alpha = 3.1$ and $\beta = 3.7$, which is in reasonable agreement with the values reported here. This model is plausible for chromium centers as well, although an experimental mapping of the phonon density of states is not feasible due to the small Huang-Rhys parameter[27] of these centers, which is on the order of 0.05.[19] That said, the variation of α and β from center to center suggests that a mechanism governed more by local rather than global properties of the material may be playing a central role in the photon dephasing.

An alternative model takes into account explicitly the impurity-rich nature of a material and incorporates the effect of phonons to the coupling of the centers (e.g., Coulombic and

spin dipolar) to nearby lattice impurities and other centers.[28] Consequently, a time-varying potential at the location of a center leads to a T^3 dependence of the dephasing rate, valid for the temperature range $T_0 < T < T_D$, with T_D being the Debye temperature and $T_0 = c^{3/8} T_D$. The coefficient c is the impurity concentration in the host crystal. Applying this general principle to the chromium emitters, an impurity concentration as high as 1 part per million gives $T_0 \sim 10$ K and $T_D = 1850$ K for diamond, so the temperature regime over which the chromium centers are investigated lies within this range. The presence of charges in the immediate environment of the emitter is already evident from the slow-wandering-type decay of coherence exhibited by some of the centers [Gaussian coherence profile in Fig. 2(a)]. This confirms the plausibility of such a dephasing mechanism. Further investigation of the temperature-dependent dephasing as a function of concentration c of defects is necessary for an unambiguous identification of the dephasing type.

IV. TEMPERATURE DEPENDENCE OF ZPL INTENSITY

Coupling of a color center to a vibronic mode also leads to reduced ZPL intensity with increasing temperature:[16,27,29]

$$I_0(T) = I_0(0) \exp\left[-S \coth\left(\frac{\hbar\omega}{2k_B T}\right)\right] J_0\left[S \operatorname{csch}\left(\frac{\hbar\omega}{2k_B T}\right)\right], \tag{1}$$

where I_0 is the fraction of emission intensity decaying into the ZPL, S is the Huang-Rhys factor, ω is the vibronic mode frequency, $\hbar$ is the reduced Planck constant, k_B is the Boltzmann constant, and J_0 is the zeroth-order Bessel function of the first kind. For chromium centers $S < 0.05$,[19] and $\hbar\omega$ is on the order of about 10 meV, similar to other diamond centers.[3,10,16] Equation (1) applied to chromium centers yields 95% of the ZPL intensity to be sustained within the temperature range we study here. In strong contrast, Fig. 4(a) displays the significantly more rapid reduction of the ZPL intensity observed as a function of temperature. Such a strong reduction in intensity is uncharacteristic for $S \sim 0.05$ and suggests an additional mechanism taking part.

The quantum efficiency η of a transition is determined by the presence of nonradiative channels connecting the excited and the ground states of a center and is defined as $\eta = P_r/(P_r + P_{nr})$, where P_r (P_{nr}) is the probability for a radiative (nonradiative) transition. Nonradiative channels contributing to P_{nr} can become available as a function of temperature via thermal excitation from the excited state of the center to higher-energy nonradiative states. These states can either belong to the center or be formed by the impurity density in the vicinity of the emitters. Assuming that the selection rules do not affect the thermalization process, the quantum efficiency becomes temperature dependent:

$$\eta(T) = \frac{1}{1 + g e^{-\frac{E_{\text{th}}}{k_B T}}}. \tag{2}$$

The nonradiative decay process is assumed here to have a barrier with activation energy E_{th}, and the constant $g = g_{\text{th}}/g_{\text{ex}}$ is the ratio of degeneracies between the thermally activated level and the excited state.[16] The presence of a thermal excitation mechanism to additional states is further evidenced by the bunching behavior in intensity autocorrelation measurements,[10] which appears predominantly for room-temperature measurements and is suppressed at low temperatures. Including this process, the overall intensity change of the ZPL as a function of temperature is given

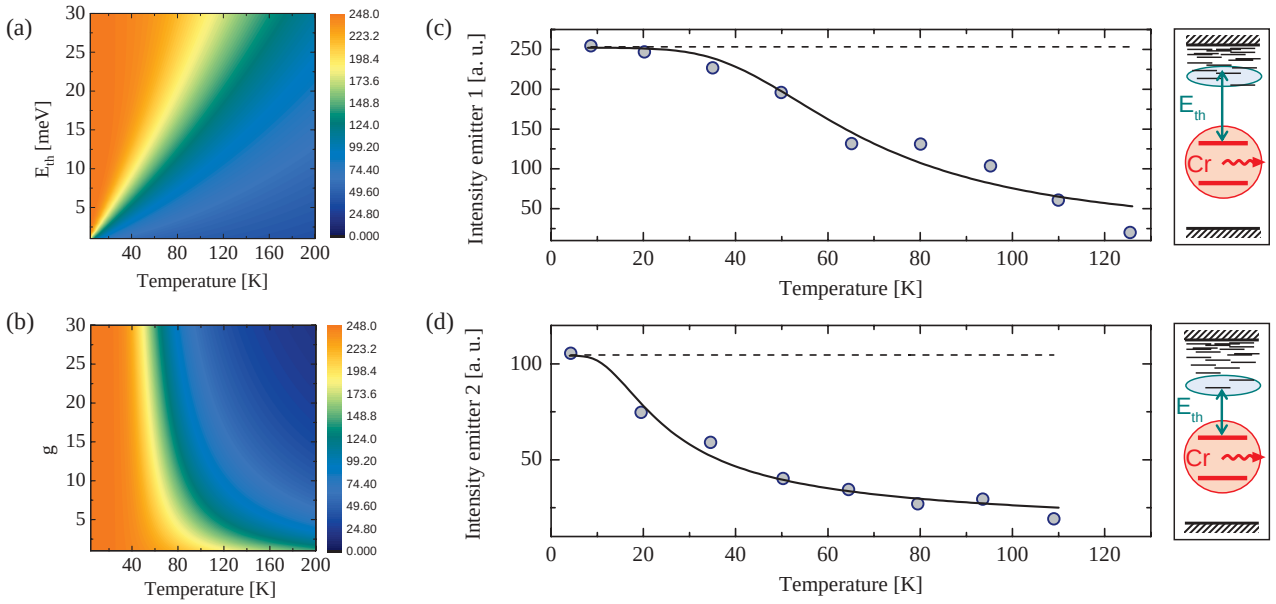

FIG. 4. (Color online) (a) and (b) ZPL intensity as a function of temperature for varying fitting parameters g and E_{th}, respectively. (c) and (d) Intensity of ZPL emission as a function of temperature for chromium emitters C and D, respectively (gray shaded circles). The black solid curves are fits to the data using Eq. (3) described in the text, and the black dashed curves give the calculated ZPL intensity in the absence of thermally activated nonradiative decay channels, according to Eq. (1) ($\hbar\omega = 10$ meV and $S = 0.05$). The side panels show the thermal coupling of the excited state to a reservoir of higher-lying states in the energy band gap. We note that the center in (c) is the same as that in Fig. 3.

TABLE I. Fit parameters for the two chromium centers shown in Fig. 4 and SiV centers for comparison.

	g	E_{th} (meV)	$\hbar\omega$ (meV)	S
Center C	19.0 ± 8	19.6 ± 3.5	28.9	0.05
Center D	4.3 ± 2	4.4 ± 1.7	28.9	0.05
SiV^0	1–3	5	28	1.5

by[16,30,31]

$$I_0(T) = \left(\frac{I(0)}{1 + g e^{\left(-\frac{E_{\text{th}}}{k_B T}\right)}}\right) \exp\left[-S \coth\left(\frac{\hbar\omega}{2k_B T}\right)\right] \times J_0\left[S \operatorname{csch}\left(\frac{\hbar\omega}{2k_B T}\right)\right]. \quad (3)$$

Figure 4(a) presents the calculated intensity of the ZPL according to Eq. (3) as a function of the number degeneracy of the state and the temperature (for a fixed value of the energy separation, E_{th} = 19.6 meV). Similarly, Fig. 4(b) presents the intensity as a function of E_{th} and temperature for a fixed value of the degeneracy, $g = 19.0$. Clearly, the intensity is sustained until the temperature is high enough to allow thermalization to be significant, and the number of the degeneracy determines how rapidly the intensity is reduced beyond this temperature. Figures 4(c) and 4(d) present experimental results (gray shaded circles) for two separate chromium centers, each superimposed on a fit using Eq. (3) (solid black curves) with E_{th} and g as fitting parameters. The corresponding values for best fits are given in Table I along with those reported for the neutral silicon-vacancy center[16] for comparison. The values for both g and E_{th} for center C displayed in Fig. 4(c) are higher than those for center D displayed in Fig. 4(d). The difference in energy separation and degeneracy of the thermally occupied states is not surprising given that the chromium emitters are known to be in an environment comprising a high density of impurity atoms, such as additional nitrogen, oxygen, and silicon.[10,19] While the model assumes thermal coupling to only one additional state, we interpret from the high values of g and E_{th} that the chromium emitters couple to an ensemble of states with an *effective* energy barrier E_{th} and an overall degeneracy ratio g. Intuitively, the number of states or the degeneracy in the ensemble is expected to increase with larger energy barriers E_{th} since the number of allowed energy states introduced by impurities around the chromium emitters should be higher closer to the valence band edge. This situation is depicted in Figs. 4(c) and 4(d). In principle, this model can be extended to include a quasicontinuum band with density of states $g(E)$ formed by the impurities at a mean energy barrier E_{th}. Straightforwardly, P_{nr} in Eq. (2) then becomes $\int g(E) \exp(-\frac{E}{k_B T}) dE$. We note that using a Gaussian density of states of finite width around a mean energy barrier and hydrogenic distribution of energy levels above E_{th} (Ref. 32) both yield similar functional dependence for intensity and linewidth of the zero-phonon transition. However, independent measurements would be necessary to reveal the location of the energy barrier per emitter, supported by a density functional theory calculations of the delocalized electronic states due to the impurities in diamond. The temperature-dependent model we use results in calculated values of 11% and 23% for the room-temperature quantum efficiency relative to the quantum efficiency at 4 K for centers C and D, respectively. These efficiencies are just below the range of measured quantum efficiencies reported in earlier work.[18] We therefore speculate that no significant temperature-independent nonradiative channels are present for these centers and that the strong suppression of thermal excitation allows quantum efficiencies at low temperatures, e.g., 4 K, of order unity.

V. CONCLUSION

In summary, the temperature dependence of photon emission from single chromium centers in diamond revealed the interplay between slow and fast dephasing mechanisms and the presence of coupling to the impurities in the vicinity of the centers. Due to these coupling mechanisms, the photon coherence times remain about 3.5 times in bulk diamond and 30 times in microcrystals below the excited state lifetime. Nonradiative losses due to thermal excitation to additional states are dominant at elevated temperatures, but the quantum efficiency of chromium centers approaches unity at low-temperature operation. Deterministic implantation of these centers in ultrapure diamond, or their controlled incorporation in high-purity CVD microdiamonds, is therefore needed to make these systems available as good-quality single-photon sources.

ACKNOWLEDGMENTS

We gratefully acknowledge financial support from the University of Cambridge and the European Research Council (FP7/2007-2013)/ERC Grant Agreement No. 209636. Z.W. and Y.X. acknowledge the USTC-Cambridge exchange program for future physicists. We thank C.-Y. Lu and C. H. H. Schulte for technical assistance, A. N. Vamivakas and E. Neu for helpful discussions, and D. McCutcheon, A. Nazir, A. Chin, and S. L. Smith for theoretical support.

[1] R. S. Sussmann, *CVD Diamond for Electronic Devices and Sensors* (Wiley, Chichester, 2009).
[2] A. D. Greentree, B. A. Fairchild, F. M. Hossain, and S. Prawer, Mater. Today **11**, 22 (2008).
[3] A. M. Zaitsev *Optical Properties of Diamond: A Data Handbook* (Springer, Berlin, 2001).
[4] A. Gruber, A. Dräbenstedt, C. Tietz, L. Fleury, J. Wrachtrup, and C. von Borczyskowski, Science **276**, 2012 (1997).
[5] J. Wrachtrup and F. Jelezko, J. Phys. Condens. Matter **18**, S807 (2006).
[6] C. L. Degen, Appl. Phys. Lett. **92**, 243111 (2008).
[7] E. Neu, D. Steinmetz, J. Riedrich-Moller, S. Gsell, M. Fischer, M. Schreck, and Ch. Becher, New J. Phys. **13**, 025012 (2011).
[8] V. A. Nadolinny, A. P. Yelisseyev, J. M. Baker, M. E. Newton, D. J. Twitchen, S. C. Lawson, O. P. Yuryeva, and B. N. Feigelson, J. Phys. Condens. Matter **11**, 7357 (1999).

[9]Y. Deshko and A. A. Gorokhovsky, Low Temp. Phys. **36**, 465 (2012).
[10]I. Aharonovich, S. Castelletto, D. A. Simpson, A. D. Greentree, and S. Prawer, Phys. Rev. A **81**, 043813 (2010).
[11]Ph. Tamarat *et al.*, Phys. Rev. Lett. **97**, 083002 (2006).
[12]T. Müller, I. Aharonovich, L. Lombez, Y. Alaverdyan, A. N. Vamivakas, S. Castelletto, F. Jelezko, J. Wrachtrup, S. Prawer, and M. Atatüre, New J. Phys. **13**, 075001 (2011).
[13]L. C. Bassett, F. J. Heremans, C. G. Yale, B. B. Buckley, and D. D. Awschalom, Phys. Rev. Lett. **107**, 266403 (2011).
[14]Radiative lifetime broadened transitions for emitters in diamond have so far been observed for the NV center in ultrapure diamond only (Ref. 11).
[15]V. M. Acosta *et al.*, Phys. Rev. Lett. **108**, 206401 (2012).
[16]U. F. S. D'Haenens-Johansson, A. M. Edmonds, B. L. Green, M. E. Newton, G. Davies, P. M. Martineau, R. U. A. Khan, and D. J. Twitchen, Phys. Rev. B **84**, 245208 (2011).
[17]I. Aharonovich, S. Castelletto, D. A. Simpson, A. Stacey, J. McCallum, A. D. Greentree, and S. Prawer, Nano Lett. **9**, 9 (2009).
[18]S. Castelletto, I. Aharonovich, B. C. Gibson, B. C. Johnson, and S. Prawer, Phys. Rev. Lett. **105**, 217403 (2010).
[19]P. Siyushev *et al.*, New J. Phys. **11**, 113029 (2009).
[20]Y. P. Varshni, Physica **34**, 149 (1967).
[21]The Varshni temperature dependence (Ref. 20) is of the form $E_g(T) = E_g(0) - aT^2/(T + b)$, where $E_g(0) = 5.4125$ eV is the diamond band gap energy at zero temperature, $a = -1.979 \times 10^{-4}$, and $b = -1437$ for bulk diamond.
[22]A. A. Maradudin, in *Solid State Physics*, Vol. 18 (Academic, New York, 1966), pp. 273–420.
[23]K.-M. C. Fu, C. Santori, P. E. Barclay, L. J. Rogers, N. B. Manson, and R. G. Beausoleil, Phys. Rev. Lett. **103**, 256404 (2009).
[24]E. Neu, C. Hepp, M. Hauschild, S. Gsell, M. Fischer, H. Sternschulte, D. Steinmueller-Nethl, M. Schreck, and C. Becher, arXiv:1210.3201.
[25]A. Halperin and O. Nawi, J. Phys. Chem. Solids **28**, 2175 (1967).
[26]H. M. J. Smith, Philos. Trans. R. Soc. London, Ser. A **241**, 105 (1948).
[27]K. Huang and A. Rhys, Proc. R. Soc. London, Ser. A **204**, 406 (1950).
[28]V. Hizhnyakov, J. Chem. Phys. **111**, 178131 (1999).
[29]G. Davies, Rep. Prog. Phys. **44**, 787 (1981).
[30]T. Feng and B. D. Schwartz, J. Appl. Phys. **73**, 1415 (1993).
[31]A. T. Collins, L. Allers, C. J. H. Wort, and G. A. Scarsbrook, Diamond Relat. Mater. **3**, 932 (1994).
[32]A. Chin and S. L. Smith (private communication).

Log in to My Ulrich's

Macquarie University Library --Select Language--

Search Workspace Ulrich's Update Admin

Enter a Title, ISSN, or search term to find journals or other periodicals:

1098-0121

Advanced Search

JCR Web ingentaconnect Article Linker

Search My Library's Catalog: ISSN Search | Title Search

Search Results

Physical Review B (Condensed Matter and Materials Physics)

Title Details | Table of Contents

Related Titles

Alternative Media Edition (3)

Lists

Marked Titles (0)

Search History

1098-0121

Save to List Email Download Print Corrections Expand All Collapse All

Basic Description

Title	Physical Review B (Condensed Matter and Materials Physics)
ISSN	1098-0121
Publisher	American Physical Society
Country	United States
Status	Active
Start Year	1893
Frequency	48 times a year
Language of Text	Text in: English
Refereed	Yes
Abstracted / Indexed	Yes
Serial Type	Journal
Content Type	Academic / Scholarly
Format	Print
Website	http://prb.aps.org/
Email	prb@aps.org
Description	Specializes in condensed-matter phenomena; covers structural phase transitions, mechanical properties and defects, dynamics, latice effects, quantum solids and liquids, magnetism, superfluidity and superconductivity.

Subject Classifications

Additional Title Details

Title History Details

Publisher & Ordering Details

Price Data

Online Availability

Other Availability

Demographics

Reviews

Save to List Email Download Print Corrections Expand All Collapse All

Contact Us | Privacy Policy | Terms and Conditions | Accessibility

Ulrichsweb.com™, Copyright © 2011 ProQuest LLC. All Rights Reserved